Raman Scattering from Semiconducting and Metallic Ge(As)†

J. Doehler,* P. J. Colwell,‡ and S. A. Solin
The Department of Physics and The James Franck Institute, The University of Chicago, Chicago, Illinois 60637
(Received 12 June 1974)

By use of an yttrium aluminum garnet laser operating at 2.1 μm, polarized transmission Raman spectra of Ge(As) have been measured for impurity concentrations spanning the Mott transition. The valley-orbit Raman line broadens markedly at the transition; its line shape has been fitted using the London-Heitler method. The spectrum in the metallic regime constitutes the first observation of single-particle scattering from intervalley fluctuations.

Though many experimental techniques, including transport[1] and spin-resonance[2] measurements, have been employed to data to study the Mott transition, none has yielded information on the role of the discrete excited electronic impurity states in the transition. In contrast, Raman-scattering measurements, when applicable, yield information on the various properties of the excited states, including the width, symmetry, and energy, and thus complement the more traditional experimental methods. Accordingly, we report here the first Raman study of the Mott transition. The subject of this study is Ge(As).

As-doped Ge is an ideal system to probe the metal-nonmetal (MNM) transition in doped semiconductors because of its large valley-orbit splitting.[3] In addition, the absorption coefficient of As-doped Ge shows[4] a sharp minimum near 2.1 μm; the crystal remains practically transparent to 2.1-μm exciting light, even in the metallic regime. Thus, the experimental setup used to record transmission Raman spectra of Ge(As) employs as its basic component an *ABC*-YAlG (yttrium aluminum garnet doped with various concentrations of Er, Tm, Ho, and Yb) laser 2.1-μm excitation source. The apparatus is similar to that described by Doehler, Colwell, and Solin[5] with one exception: The system sensitivity has been significantly improved by equipping the PbS detector with a narrow-band cold filter and cold baffles. Typical integration times have been reduced from 100 to 10 sec.

The first-order Raman spectrum of Ge doped with 6.5×10^{15} cm^{-3} As impurities is shown in Fig. 1(a). The feature at 35 cm^{-1} arises from the valley-orbit $1s(A_1)$ to the $1s(T_2)$ Raman transition; its symmetry characteristics have already been reported.[5] As the concentration is increased [Figs. 1(b)–1(e)], the line grows in magnitude while the integrated intensity remains proportional to the impurity concentration for concentrations between 6.3×10^{15} and 5.5×10^{17} cm^{-3}. At a concentration $n=5.4\times10^{16}$ cm^{-3} the line develops a tail on the low-energy side while at $n=1.7\times10^{17}$ cm^{-3} a tail also appears on the high-energy side. At $n=5.5\times10^{17}$ cm^{-3}, the linewidth is ill defined, and the spectrum acquires a new shape. It shows a broad single-particle-like continuum[6] that indicates a delocalization of states in which the electron wave functions extend over many donor sites.

The MNM transition in Ge(As) is known from conductivity measurements[7] to occur at an impurity concentration between 2.5×10^{17} and 3.0×10^{17} cm^{-3}. At $T=0$ K, the single-particle spectrum should show a sharp cutoff on the Stokes side of the laser line at $\omega_c=qV_F$, where q is the wave vector transferred during the scattering process and V_F is the Fermi velocity. At $n=5.5\times10^{17}$ cm^{-3}, 7 cm$^{-1}\leq\omega_c\leq127$ cm^{-1}. The spread reflects the effective-mass anisotropy. Though instrumental and lifetime effects and the nonzero temperature smear the spectrum of Fig. 1(j), it is consistent with the above-mentioned range of cutoff frequencies.

A number of coupling mechanisms can give rise to Raman scattering from single-particle excitations. To our knowledge, only two such mechanisms have been observed experimentally, charge-density fluctuation (CDF) coupling and spin-density fluctuation (SDF) coupling.[6] The former is observable only in the parallel-polarization configuration, whereas the latter is observable only in the crossed-polarization configuration. With a judicious choice of crystal axis orientation and polarization configuration, the single-particle CDF and/or SDF contributions to the Raman spectra can be separated from the valley-orbit contribution. However, light scattering from intervalley fluctuations,[8,9] which has not

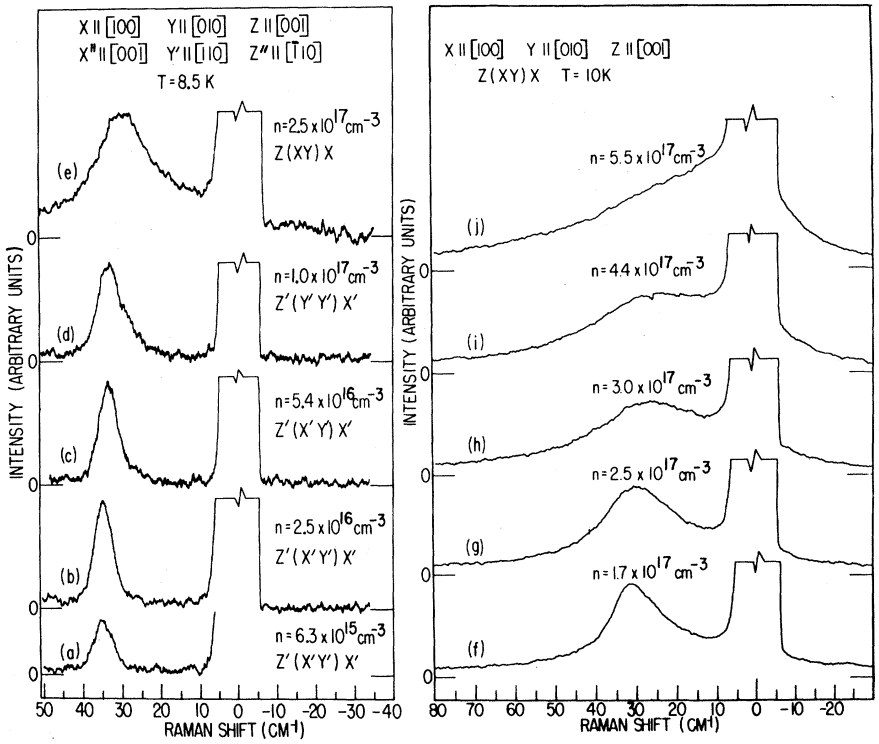

FIG. 1. Raman spectra of As-doped Ge as a function of impurity concentration. The system gain for spectra (a) to (e) was approximately twice the gain for spectra (f) to (j). The abscissa is linear in wavelength rather than wave number.

been previously observed, has been predicted to have the same polarization selection rules as the valley-orbit Raman line. Our measurements indicate that the single-particle spectrum of Ge(As) does indeed have polarization properties identical to those of the valley-orbit line and is not due to either CDF or SDF, but to intervalley fluctuations.

The line shapes at $n = 1.7\times10^{17}$ and 2.5×10^{17} cm^{-3} [Figs. 1(f) and 1(g)] are particularly interesting because they suggest that the spectra consist of a broadened valley-orbit line superimposed upon a single-particle spectrum, the single-particle spectra being similar in shape to the spectrum for $n = 5.5\times10^{17}$ cm^{-3} but uniformly reduced in amplitude. The existence of the background, therefore, indicates that a substantial fraction of the electrons are delocalized even at a concentration level below n_c. The existence of anti-Stokes scattering is also an indication of delocalized electrons. Note that the peak of the valley-orbit line moves to *lower* wave-number shifts as the concentration is increased, even above n_c. If the spectra for $n > n_c$ were due only to free electrons, we would expect the peak to move to *higher* wave-number shifts as the concentration is increased since the characteristic frequency, ω_c, is proportional to $n^{1/3}$. The data of Fig. 1(f) were taken at a temperature at which metallic conduction is observed in high-concentration samples.[7] For such samples, the electrons are delocalized within the "impurity band." Note that the dc conductivity for $n = 1.7\times10^{17}$ cm^{-3} is still characteristic of a semiconductor.[7]

In order to explain the concentration dependence of the line shapes observed in Fig. 1, we apply the Heitler-London (H-L) method (for calculating the dependence of the ground-state splitting on the separation of a pair of hydrogen atoms) to As impurities in germanium.[10] H-L showed that as two hydrogen atoms are brought together, the 1*s* ground states split into a symmetric (bonding) state and an antisymmetric (antibonding) state, the energies of which can be calculated exactly. In the effective-mass approximation, the ground-state wave function of the As impurity has a hydrogenic 1*s* envelope. Therefore, we assume that the H-L method is also applicable to As impurities in Ge provided we correct for the dielectric constant and for the effective masses appro-

priate to the host crystal. In this approximation, the $1s(A_1)$ and the $1s(T_2)$ states behave in the same fashion. Clearly, the $1s$ states of Ge(As) will broaden as will the valley-orbit Raman line if there is a distribution of interparticle As-As distances. Let $E_A(r)$ and $E_B(r)$ be the energies of the As antibonding and bonding states, respectively. $E_A(r)$ is a positive, monotonically decreasing function of r while $E_B(r)$ exhibits a well-known negative minimum at $r_0 \cong 1.5a_H$, where a_H is the Bohr radius. Both functions tend to 0 as $r \to \infty$. Let $r(\omega)$ be the inverse function, defined as the value of $r \geq r_0$ for which $E_A(r) = \omega$ or $E_B(r) = \omega$. The function is single-valued for $r \geq r_0$, the region of interest, and defined on the interval $E_B(r_0) \leq \omega \leq E_A(r_0)$. Let us now assume a Poisson distribution in the As-As interparticle distances.[11] The probability of not finding a neighbor closer than r is given by

$$P(r) = \exp[-(4\pi n/3)r^3]. \quad (1)$$

The probability of finding a neighbor within r and $r+dr$ is then equal to $-(dP/dr)\,dr$, i.e., dP/dr is proportional to the pair distribution function $G(r)$. The density of states $\mathfrak{D}(\omega)$ in the $1s(A_1)$ "band" is then given by

$$\mathfrak{D}(\omega)\,d\omega \propto P(r(\omega)) - P(r(\omega + d\omega)) \quad (2)$$

or

$$\mathfrak{D}(\omega) \propto G(r(\omega))\,dr/d\omega. \quad (3)$$

Since the density of states in the $1s(T_2)$ "band" is assumed to be identical to that in the $1s(A_1)$ "band," the valley-orbit line shape is given by the joint density of states:

$$I_{vo}(\omega) \propto \int \mathfrak{D}(t)\mathfrak{D}(t - \omega + 4\Delta)\,dt, \quad (4)$$

4Δ being the valley-orbit splitting. The line shape thus calculated is symmetric whereas the measured line shape shown, for example, in Fig. 1(g) is asymmetric. Therefore, the asymmetric background has to be taken into account explicitly.

The single-particle spectrum for $n = 2.5 \times 10^{17}$ cm^{-3} will have a shape quite similar to that for $n = 5.5 \times 10^{17}$ cm^{-3} because ω_c varies only as $n^{1/3}$. Let $I_M(\omega)$ represent the spectrum shown in Fig. 1(j). We have attempted to fit the line shape in Figs. 1(f)–1(i) using the following function:

$$I(\omega) = aI_{vo}^{c}(\omega) + bI_M(\omega), \quad (5)$$

where $I_{vo}^{c}(\omega)$ is $I_{vo}(\omega)$ convolved with the spectrum shown in Fig. 1(a) to account for instrumental and lifetime broadening; a and b are adjustable parameters. The result is shown in Fig. 2. In Fig. 2(b), a, b, the Bohr radius, and the valley-orbit splitting are adjustable parameters. The optimum Bohr radius was 27 Å in good agreement with the effective Bohr radius given by $(a_H)_{eff} = (a_H)_{e.m.}[E_{obs}/E_{e.m.}]^{1/2}[n_s/n]^{1/3} = 28.5$ Å. Here E_{obs} ($E_{e.m.}$) is the observed (effective-mass) binding energy and n_s is the effective semiconducting concentration defined by Mikoshiba.[11] The fits to the line shapes shown in Figs. 2(a), 2(c), and 2(d) were obtained by leaving the Bohr radius fixed at 27 Å. Also shown in Fig. 2(b) is the best fit to the line shape of Fig. 1(g), assuming only a valley-orbit contribution to the Raman intensity. Though the fits to the line shapes of Fig. 2 involve at least three adjustable parameters, none of the spectra of that figure can be successfully fitted without the inclusion of both valley-orbit and single-particle scattering contributions to the Raman intensity. Nevertheless at higher concentrations, clusters containing more than two As atoms will certainly contribute to the linewidth of the valley-orbit components. Thus the H-L approximation described above probably underestimates the linewidth at higher concentrations.

In conclusion, the MNM transition has been the subject of considerable recent theoretical controversy between Mott[12] on the one hand and Cohen and Jortner[13] (CJ) on the other. In Mott's model,[14] the valley-orbit line would be homogeneously broadened by the temporal fluctuations of the mo-

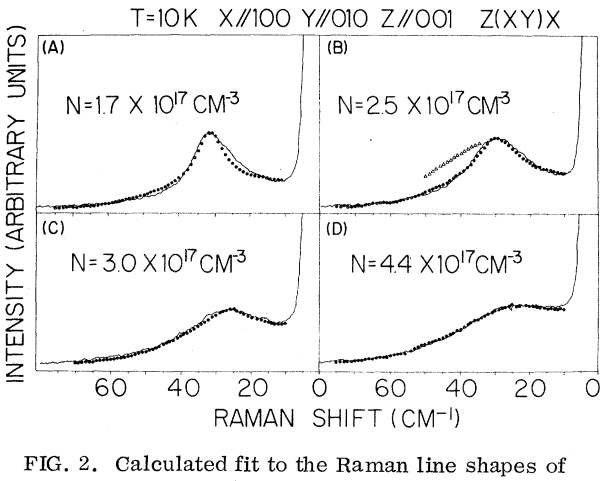

FIG. 2. Calculated fit to the Raman line shapes of Ge(As) shown in Fig. 1 assuming, for the circles; valley-orbit superimposed upon a single-particle background; for the triangles, only a valley-orbit contribution. Note that the abscissa is linear in wavelength rather than wave number.

mentarily singly occupied donor sites, fluctuations which are expected to occur in the highly correlated electron gas.[15] In the CJ model, density fluctuations produce an inhomogeneous broadening of the valley-orbit line. Although the crude calculations described above are based on density fluctuations and therefore seem to favor the CJ model, the observed Raman line shapes might be fitted equally well by assuming the existence of only temporal fluctuations. Hopefully, our Raman data coupled with a more sophisticated theoretical interpretation will serve to distinquish between the models of Mott and CJ.

We wish to thank H. Fritzsche and A. K. Ramdas for the use of their samples and M. H. Cohen for helpful discussions. We are particularly grateful to M. V. Klein for bringing to our attention the intervalley fluctuation mechanism.

†Work supported by the U. S. Atomic Energy Commission and in part by the National Science Foundation and the Louis Block Fund of The University of Chicago.

*Present address: Bell Laboratories, Holmdel, N. J. 07733.

‡Present address: Department of Physics, Michigan State University, East Lansing, Mich. 48823.

[1]G. Busch and H. Labhart, Helv. Phys. Acta 19, 463 (1946).

[2]G. Feher, Phys. Rev. 114, 1219 (1959).

[3]J. H. Reuszer and P. Fisher, Phys. Rev. 135, A1125 (1964).

[4]J. I. Pankove and P. Aigrain, Phys. Rev. 126, 956 (1962).

[5]J. Doehler, P. J. Colwell, and S. A. Solin, Phys. Rev. B 9, 636 (1973).

[6]For a review of the properties of solid state plasmas and of light scattering from single-particle excitations, see, for example, P. M. Platzman and P. A. Wolff, in *Waves and Interactions in Solid State Plasmas*, Suppl. No. 13 to *Solid State Physics*, edited by H. Ehrenreich, S. Seitz, and D. Turnbull (Academic, New York, 1973).

[7]H. Fritzsche, Phys. Rev. 125, 1552 (1962).

[8]P. M. Platzman, Phys. Rev. 139, A379 (1965).

[9]S. V. Gantsevich, V. L. Gurevich, V. D. Kagan, and R. Katilius, in *Proceedings of the Second International Conference on Light Scattering in Solids*, edited by M. Balkanski (Flammarion Sciences, Paris, 1971), p. 94.

[10]W. Heitler and F. London, Z. Phys. 44, 455 (1927).

[11]N. Mikoshiba, Rev. Mod. Phys. 40, 833 (1968).

[12]N. F. Mott. Phys. Rev. Lett. 31, 466 (1973).

[13]M. H. Cohen and J. Jortner, Phys. Rev. Lett. 30, 699 (1973).

[14]N. F. Mott. Contemp. Phys. 14, 401 (1973).

[15]W. F. Brinkman and T. M. Rice, Phys. Rev. B 2, 4302 (1970).

Magnetic Excitations and Magnetic Ordering in Praseodymium

J. G. Houmann, M. Chapellier,* and A. R. Mackintosh
Danish Atomic Energy Research Establishment, Risø, Denmark

and

P. Bak
Danish Atomic Energy Research Establishment, Risø, Denmark, and Brookhaven National Laboratory, Upton, New York 11973

and

O. D. McMasters and K. A. Gschneidner, Jr.
Ames Laboratory–USAEC and Department of Metallurgy, Iowa State University, Ames, Iowa 50010

(Received 9 December 1974)

The dispersion relations for magnetic excitons propagating on the hexagonal sites of double-hcp Pr provide clear evidence for a pronounced anisotropy in the exchange. The energy of the excitations decreases rapidly as the temperature is lowered, but becomes almost constant below about 7 K, in agreement with a random-phase-approximation calculation. No evidence of magnetic ordering has been observed above 0.4 K, although the exchange is close to the critical value necessary for an antiferromagnetic state.

For a number of years there has been a controversy about the existence of magnetic ordering in Pr, the only element to display the characteristic magnetic behavior of a singlet ground-state system with weak exchange interactions. An antiferromagnetic structure below a Néel tempera-